



# EUREC Agency

European Master in Renewable Energy

---

Academic year 2003-2004

***Title:* Architectural PV solar modules production line:  
Process description and implementation**

**Full Name of Student:** José María Román Faúndez

**Core Provider:** CIRCE, CPS, Universidad de Zaragoza, Zaragoza, Spain

**Specialization:** NPAC, Northumbria University, Newcastle, UK

**Host Organization:** Romag Ltd., Consett, Co. Durham, UK

**Academic Supervisor:** Ignacio Zabalza Bribián

**Specialist Supervisor:** Nicola Pearsall

**On – site supervisor:** Kevin Webster

**Submission Date:** September 24<sup>th</sup>, 2004



# **Architectural PV solar modules production line: Process description and implementation**

*José María Román Faúndez*

*CIRCE  
Centro Politécnico Superior  
Universidad de Zaragoza  
C/ María de Luna 3  
E-50015 Zaragoza  
Spain*

*and*

*Romag Ltd.  
Leadgate Industrial Estate  
Consett, Co. Durham, DH8 7RS  
United Kingdom*

## **Abstract**

This report presents the start-up of the 6MW<sub>p</sub> PV module production line for custom-made architectural glass-glass modules at Romag Ltd. The commissioning of the equipment started in May 2004 and has been installed, tested and set for production since then, to which the candidate has contributed actively. Environmental and socio-economic factors are driving the market growth of Renewable Energy Sources and PV in particular. A general introduction to the main features and performance of solar cells, modules and systems is also offered to make more comprehensible the process definition of the production line. Every piece of equipment forming the production line is briefly described and the process outlined, starting with the cell stringing, module assembly, lamination and testing of electrical performance. A major emphasis is given to the lamination process, where the contribution by the candidate has been more relevant.

**Keywords:** Glass-glass PV modules, EVA lamination process, automated PV production line.

## Acknowledgements

Resulta curioso recordar cuando era más joven e iba a visitar a mi abuelo, que siempre se quejaba sobre el tiempo, porque le estropeaba la cosecha de garbanzos, cerezas..., siempre iba a ser buenísima hasta que venía la canícula, las heladas..., y yo pensaba que tenía que dedicarme a alguna profesión diferente de la agricultura para no depender de los avatares del tiempo. Y ahora, a la vuelta de los años, mi dependencia de las condiciones climatológicas es la misma, y más en el lugar donde he ido a parar, Newcastle, 55° north, not a bad place... if it wasn't for the weather. Después de todo parece que no hemos avanzado tanto en dos generaciones.

En cualquier caso debo empezar estos agradecimientos por mi madre, que ha vuelto a dejarme marchar lejos sin protestar demasiado; será porque no son 7000 km esta vez. De todas formas ya veré cuando vuelvo, porque creo que de esta me cuelga.

A quién realmente tengo mucho que agradecer, no solo porque me haya dejado marchar, si no porque me haya ayudado muchísimo en mi empeño, por no hablar de los últimos años, es a Germán Sierra. Gracias a su ayuda pude llegar a Zaragoza e integrarme rápidamente, casi como si fuera mi casa. Allí recibí la bienvenida de todo el departamento de Física Teórica (yo es que soy físico teórico, para aquellos que no lo sepan, a pesar de que ahora me dedique a tostar paneles solares en un "horno"; según mis hermanos se me nota en la cara, y si ellos lo dicen...), en particular quiero destacar a Fernando Falceto, José Esteve, Manolo Asorey, José Luis Alonso y Julio Abad. Aunque a veces no lo parezca, un departamento de física es buen sitio para conocer gente; así tuve la oportunidad de conocer a Pierpaolo Bruscolini, con quién pasé muy buenos momentos. Jesús Montenegro y Antonio, muy andaluz el primero, no mucho el segundo, mis compañeros de piso, también me acogieron muy bien, como toda la ciudad de Zaragoza en general, ¡nada más llegar hicieron una fiesta!, ¿qué más se puede pedir? La verdad es que repetiré, porque las fiestas del Pilar son para vivirlas.

Luego, en medio de tan buen ambiente no podía faltar un buen curso y unos compañeros de clase superentusiastas. Aunque parezca peloteo, no quiero dejar pasar la ocasión de agradecer a nuestros profesores, Alfonso Aranda, Ignacio Zabalza, Sabina Scarpellini, Fernando Sebastián..., las clases recibidas y los buenos momentos, sobretodo con Alfonso. También los hubo no tan buenos, y si no solo hay que mentar a Pinilla, pero entre todos conseguimos sobreponernos y no tuvimos que utilizar "la regla del CIRCE". Los que lo pasamos muy bien, a pesar de todo el trabajo que nos daban, éramos los sufridores, ahí va la lista: Adrián Mate, Albert Masés, Alessandro Scrivani, tan italiano que actúa de embajador allá donde va, Amado Pérez, el Tercer Hombre en Alemania, Emma Dayan, la Principessa, Javier de la Torre, Jérôme Jarlang, the off-shore man, con proyectos increíbles y entusiasmo para llevarlos a cabo, dar y tomar, y Samuel Delobbe, y Sabrina también, que no se nos olvide. Desde luego, es un placer conocer a gente así.

After such a good time in Zaragoza I could not imagine that things were going to be even better in Newcastle. Right from the very beginning I found all the people in the university very kind and helpful, starting with the teachers, Kathleen Hynes

and Nicola Pearsall, and the Graduate Students, Thomas Bauer and Jaya Ramachandran. My first days in Newcastle were very strange, although this is not the place to write about them I want to say thank you to all the people who helped me to adjust fast enough not to want to go back home after the first week: The Balmoral Terrace mafia, Patera and Jovian, Miguel Lamas, Tania Radeva, John Short, and so many others, Alicia Magro, just like my daughter, Karim Ziyad and the twins with the Chillingham Rd. parties, and ... Tina, our muse; my housemates Rob Williams, a big boy who coming from Swansea (Wales) thought this was Newcastle, New South Wales, Australia, Joe Heathcote and Adam Baker, the English part of the gang, and Amanda Holly, this, definitively, Australian herself. But above all I want to thank my classmates, without whom this stay would have been a painful experience, but at the same time the last months of the project module would have been easier, as I would not have been remembering the passed good times that I am not having anymore, sniff, sniff. Thank you all, Keith Boyle, always devising something to do during the weekends, weekends have been so dull since you are gone; Rodrigo Ruiz, good memory with salsa steps and always on the phone; Susana Fernández and Quili Capellín, the Asturian connexion, always happy, smiling and ready to have a fabada; and Emma Dayan, again, as she also came to such a “good” place for Photovoltaics, lived in Balmoral Terrace, stayed longer, and went away closer (to Winchester), I don’t know if for good or not so good.

And what can I say about people at Romag? I have been treated so well from the first day that made me almost suspicious. With Kevin Webster, Peter McQueen, Joe Paisley (“tonite we go to the toon”), Keith Morrison and Jason Ledger (sure he misses trimming the EVA now that he is fighting the stringer) I managed to learn some Geordie phrases like “noon, toon, broon, fall, doon, in the undergroon”; everybody laughs when I say it, I wonder why... I learnt this and more even from those who are from farther north, like Phil Wilson with whom I rode the bus everyday to Leadgate, such a nice place! I would like to thank José Luis Corbacho, María José Valenzuela, and Ana Ortigao from BP Solar in Madrid for their welcome and all the information I obtained from them. Oh man!, it made sense of all the chaotic and incomprehensible material that Rob Miles tried to teach us without success.

Ahora ya solo queda utilizar todo lo que hemos aprendido para hacer de éste un mundo mejor, aunque no lo merezca, porque ni siquiera Antonio Valero ha conseguido minar nuestro ánimo hasta el punto de desear utilizar la famosa regla del CIRCE. Así que es hora de poner en práctica la frase de guerra que teníamos en Zaragoza:

*Venga, vamos, a por ellos...*

## Table of contents

Acknowledgements.....	4
Table of contents .....	6
List of figures .....	6
1 Introduction.....	7
2 Factors for the promotion of Renewable Energy Sources .....	8
2.1 Added value of building integrated PV systems .....	9
3 Man-made solar energy conversion systems .....	10
3.1 Solar cells.....	10
3.1.1 Types of solar cells .....	11
3.1.2 Fundamentals of solar cells .....	13
3.2 Solar modules .....	17
3.2.1 Glass-glass modules produced by Romag Ltd.....	18
3.3 Solar systems: Building Integrated Photovoltaic Systems (BIPV) ...	21
4 Production line description .....	23
4.1 Cell tester .....	24
4.2 Tabber and stringer .....	25
4.3 String handler .....	27
4.4 Bus bars soldering.....	28
4.5 Laminator .....	28
4.6 Flash-tester .....	29
5 Lamination process .....	30
5.1 Physical and chemical properties of EVA.....	31
5.2 Lamination cycle definition .....	33
6 Conclusions and prospects .....	35
References .....	36

## List of figures

Figure 1: Solar spectrum before and after crossing the atmosphere.....	11
Figure 2: Monocrystalline and polycrystalline silicon solar cells. ....	12
Figure 3: I-V characteristics for a solar cell. ....	14
Figure 4: I-V characteristics dependence on light intensity. ....	15
Figure 5: I-V characteristics dependence on temperature.....	15
Figure 6: I-V characteristics dependence on series resistance. ....	16
Figure 7: I-V characteristics for a series configuration.....	17
Figure 8: Shaded cell by-pass diode. ....	18
Figure 9: I-V characteristics for parallel configuration.....	18
Figure 10: Single-glazing construction, Gateshead modules. ....	19
Figure 11: I-V characteristics for Gateshead module. ....	20
Figure 12: Double-glazing construction, Falstone modules.....	21
Figure 13: Stand-alone system diagram.....	22
Figure 14: Grid-connected system diagram. ....	22
Figure 15: Tabber and stringer diagram. ....	26
Figure 16: String handler diagram.....	27
Figure 17: Laminator diagram. ....	29
Figure 18: Lamination process cycle parameters. ....	34

# 1 Introduction

Romag Ltd. is a leading UK based glass processor serving the architectural, security and specialist transport sectors. Increasingly, glass for buildings needs to perform several functions, not only providing a means to see outside and allow light into the building. In most situations glass is used as a structural component, and has to provide insulation to keep the heat in, as well as out of the building. The processing of the glass is based on three processes, namely, lamination, toughening and bending. The expansion of the architectural sector of the business to the production of PowerGlaz Building Integrated Photovoltaic Glass is a logical step in the present growing PV market.

This PowerGlaz is installed in façades of buildings, replacing conventional glazing materials at the same time as producing energy from the daylight, and plays a very important role promoting the awareness of the general public of the present state of the technology and its dissemination to a larger scale, which, in turn, will contribute, through an increment in the production, to a reduction in cost of cells and modules. This is possible because a higher throughput leads to an improvement of the equipment for handling and producing modules, gaining experience through a learning curve. The Photovoltaic Manufacturing Technology Program (PVMaT Program) started in the USA is obtaining good results [1, 2, 3, 4, 5, 6].

This report presents the start-up of the 6MW<sub>p</sub> PV module production line for custom-made architectural modules at Romag Ltd. The commissioning of the equipment started in May 2004 and has been installed, tested and set for production since then. This is a time consuming task as not all the equipment has been set up at the same time, and there are still pieces of equipment not installed. The candidate has contributed actively in the setting of every piece of equipment and the implementation of the whole production process, from the design of the modules to the testing of their performance. Since every order comprises a different number of modules and different module sizes and cell layout the process definition is quite slow, as new complications and problems appear with each order produced.

This is a good moment to invest in a module production line, since several factors are contributing to the governmental promotion of Renewable Energy Sources (RES) in general, and Photovoltaic (PV) Solar energy in particular. Section 2 is devoted to briefly outline the environmental and socio-economic reasons in favor of this promotion as compared with the traditional fossil-fuel energy sources. Advantages of the introduction of PV elements integrated in the building structures are presented as well.

In Section 3 the solar production systems are presented, leading the reader through the basic structure and main features of solar cells, modules, and whole systems, the ones producing and delivering the energy to the loads. Structural details for some of the first modules produced by Romag Ltd. are presented in this section.

A step by step tour of the module production line is carried out in Section 4, where every piece of equipment and stage of the process is considered to some extent, namely, cell stringing, electric interconnection of the strings and module

assembly, lamination process and flash testing of the finished module [2-4, 7, 8, 9, 10]. Due to the fact that some of the information, particularly regarding technical data for the process definition, is considered proprietary information by the company, only general ideas, and methods in the definition of the process are presented. However, the fact that the modules have been produced (output data is presented for some of the modules) and delivered to the customer ensures that the process is running and working to a satisfactory level.

The most detailed approach is taken when establishing the lamination process, since this is the most delicate stage of the process and corresponds to the highest contribution by the candidate. Lamination process definition is explained in Section 5, where a systematic approach for obtaining the laminating process is presented, but again without offering data of the parameters involved in the process beyond the general information that can be, anyway, found in the literature [11, 12].

Conclusions and prospects for future work and improvement of the process in the production line are laid in the last section, Section 6.

## **2 Factors for the promotion of Renewable Energy Sources**

Following the lines established in the Kyoto Protocol, agreed in 1997, for the reduction of emissions by 2010 of green house effect gases, like CO<sub>2</sub>, NO<sub>x</sub>..., to the levels of 1990, the EU and member states are promoting the expansion of Renewable Energy Sources (RES). The White Paper on Energy for the Future: Renewable Sources of Energy (1997) calls for a 12% share of the inland consumed energy from RES, which will equate to a 22% of the electricity consumed.

Renewable Energy Sources are considered all those coming directly or indirectly from the sun, with a balanced or favorable emission of CO<sub>2</sub>, NO<sub>x</sub> and other green house effect gases. The list is the following: Photovoltaic Solar Energy, Thermo-solar Energy, Wind Power, Hydroelectric Power, Wave Power, Tidal Power, Geo-thermal and Biomass. Biomass is considered a RES since during the growth of the crop or wood these plants have fixed the CO<sub>2</sub> which will be liberated later when burned to produce energy. From the administrative point of view, although not a RES, the Combined Heat and Power (CHP) generation is favorably treated, since it doubles the efficiency of the extraction of energy [13].

In addition to the environmental threads, nowadays 50% of the energy consumption in the European Union is coming from third countries, and this shear is expected to grow to 75% within the following 20-30 years if nothing is done. The primary energy consumption is based on fossil fuels, oil, coal and gas, with a 77% of the total energy used [13]. As most of the resources are based in very limited regions, e.g., 45% of the oil is coming from the Middle East and 40% of the gas from Russian Federation, this poses a risk to the supply of energy in the future, as mentioned in the Green Paper on Towards a European Strategy for the Security of Energy Supply (2001). RES can help to mitigate this external dependency, since they are based on local resources.



In the midst of these concerns for the environment and the necessity to ensure the future supply of energy, the EU and member states have launched a continuous campaign since the end of the 1990s to promote RES. The first program was the Campaign for Take-off (1999-2003), which has provided incentives for the installation of renewable energy power stations and facilities, particularly small scale ones, favoring diversification and decentralization of the generation. This program has been continued by the Public Awareness Campaign for an Energy Sustainable Europe (2004-2007), which aims for the increment familiarity of society with RES and the spread of awareness about the need for a more efficient energy consumption.

Some concrete targets of the above mentioned promotion schemes are the installation of one million PV systems, half of them in Europe and the other half for exporting, and a total power installed by 2010 of 3GW<sub>p</sub> from PV systems or 40GW from wind power. In order to meet this objective the PV market must grow at an annual rate of 30%, and the wind power a 10%.

This growth rates are only achievable if the RES are heavily supported by governmental authorities. This support for RES is viewed as incompatible with current trends in liberalization of the energy market [14, 15, 16], which aims to open markets to competition and to give a wider offer to customers. People in favor of this liberalization within the renewable energy sector, however, are asking for a *level playing field* where all the hidden costs of energy generation are taken into account, mainly the environmental pollution, and are pressing for polluters to pay. This way, positive or neutral environmental benefits have an increasing market value.

The way of comparing a conventional generation plant with a generation from a RES is by means of the Life Cycle Cost (LCC) method, which consists in determining the cost not just for construction and operation of the power plant, but also for the extraction, transportation, and treatment of fuel, as well as decommissioning costs at the end of the life cycle. We have also to add the risk of price fluctuations and security of supply due to geo-political and economical situations. The CO<sub>2</sub> and other chemicals liberated to the atmosphere are also responsible for further environmental damage, which needs to be accounted for. RES are hindered by their high initial capital investment. However, the recurrent cost for fuel and maintenance are very low. On the other hand, a fossil fuel plant requires a lower initial capital investment, but recurrent fuel costs are high. A LCC study of RES spreads the high initial investment over the lifetime of the system, which allows for a more faithful comparison of different technologies, favoring investment in RES in most cases.

## **2.1 Added value of building integrated PV systems**

The interest on PV systems which started in the 1970s due to the oil crisis, driven by security of energy supply, and in the 1980s and 1990s as a means for tackling environmental problems, it is now shifting its weight from the electrification of remote areas to building integrated systems (BIPV) feeding to the grid. All this provides us a large range of incentives for PV systems.

In addition to being environmentally friendly, PV systems offer non-energetic added values [17, 18] for every player in the market. For customers it reduces the cost of energy, and the modularity of the system allows for a fast installation or upgrade, then easily matching the demand. For society, the decentralized character of PV systems allows for diversification of energy supply, ensuring the energy supply. The maintenance required spurs job creation, fixing population in the rural areas. And for utilities this decentralized systems reduces times for construction of large power plants, and favors savings by supporting the grid in remote areas, avoiding expensive grid upgrades, at the same time reducing transmission and distribution losses. Moreover, utilities serving PV generated electricity benefit from a *green image*, which increases their credibility among customer groups.

Building integrated PV systems have their own advantages, by substituting cladding on the façades, or introducing novel shading systems from the architectural point of view, as with the glass-glass modules to replace windows. All this replacement reduces building cost, due to the shearing costs of construction materials and PV modules. In addition the fact that this can be in the urban environment leads to urban renewal.

Putting all this together with the LCC analysis, previously mentioned, and the other socio-economic and environmental factors, the gap between conventional energy generation and PV generation is reduced, or even favors investment in PV systems and RES in general, in comparison with fossil fuel based generation technologies

### **3 Man-made solar energy conversion systems**

Photovoltaic solar systems are based on the conversion of light into electricity. These systems can be considered at various levels. The basic component is the solar cell, which directly converts the light received from the sun into electricity. A set of cells is electrically connected and encapsulated to form the solar module, which serves as the basic component for solar systems. A solar system consists of an array of series and/or parallel connected solar modules plus a number of other elements, known as Balance of System (BOS), as a regulator, maximum power point tracking device and an inverter, which allows it to generate power from light and deliver it to a load, or the grid.

#### **3.1 Solar cells**

Solar cells are made of semiconductor materials with a band gap of 1.0-2.0eV, with an optimum band gap of 1.5eV, between its valence and conduction bands across which electrons can be excited by photons coming from the sun [19, 20]. This range of band gaps is suitable for solar cell production because they fit the emission spectrum of the sun, qualitatively described as the black-body emission spectrum at a temperature of 6000K, with a maximum emission intensity in the green color of the electromagnetic spectrum ~2.5eV (all the photons with higher energy than the band gap are susceptible of being absorbed). Figure 1 shows the precise spectral distribution of the sun outside the Earth atmosphere (AM0), with an intensity

of  $1367\text{W/m}^2$ , and at the surface of the Earth (AM1.5), after crossing different layers of the atmosphere, where an intensity of  $500\text{-}1000\text{W/m}^2$  arrives, since part of the radiation is absorbed by gases in the atmosphere and does not reach the surface of the Earth. AM denotes the Air Mass that the light travels through the atmosphere; a perpendicular ray of light crosses one atmosphere, and has a AM1 spectrum on the Earth surface. The cell performance output is offered at Standard Test Conditions (STC):  $1000\text{W/m}^2$  of a global AM1.5 spectrum at  $25^\circ\text{C}$ .

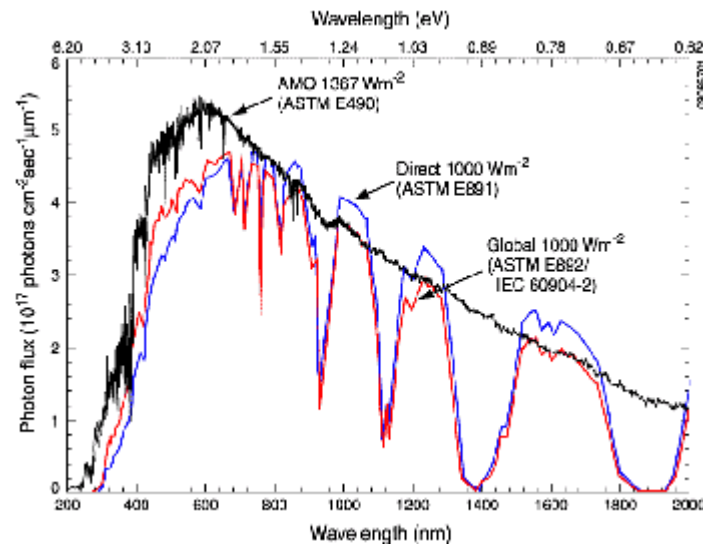


*Figure 1: Solar spectrum before and after crossing the atmosphere. The absorption of some energies in the atmosphere produces the depressions for the surface radiation. Standard Test Conditions (STC) use  $1000\text{W/m}^2$  of a global AM1.5 spectrum at  $25^\circ\text{C}$ .*

In order to generate a current it is not sufficient for a single semiconductor device, but a junction of two semiconductors with an opposite electric character, one doped negatively and one doped positively, which creates a voltage step across the junction. When a photon excites an electron across the semiconductor energy gap this electron is swept away from the junction by the electric field generated by the potential difference at both sides of the junction. Only if this electron manages to escape the cell, and is injected into an external lead an electric current is generated. Sources of recombination, like back and front surface recombination, impurities, or domain boundaries must be passivated for a better performance of the cell.

### 3.1.1 Types of solar cells

The most extensively used semiconductor material for solar cells is silicon (with a gap  $1.12\text{eV}$ ), because of its abundance, and the knowledge in handling and manufacturing pure enough ingots for the microprocessor industry. The different electric character is obtained by doping a silicon wafer with different elements, namely, n-type silicon (doped with P) and p-type silicon (doped with B). Silicon crystalline semiconductors are usually grown from the molten state, and the removal of impurities from the silicon is a delicate process. Some elements are more difficult to remove than others. This difficulty is measured by the “segregation coefficient”, which determines the relative affinity of an element for the crystalline and molten

state. For example Boron has a segregation coefficient of 0.8, while Phosphorous one is 0.35. Thus the initial ingot of silicon is positively doped and only during the cell production stage P is thermally diffused on one of the faces (the one which will become the front face of the silicon solar cell), which introduces a compensation doping changing the electrical character of that face to n-type [19, 20, 21].

In order to improve the efficiency of the cell front face this is etched producing a texture which traps the light, an antireflective coating of  $\text{SiO}_2$  or  $\text{SiN}$  is also applied. A technique known as back surface field (BSF) is applied to the back face in order to reduce the number of carriers near the surface, reducing the surface recombination. Finally electric contacts are applied in the forms of a grid to the front of the cells (trying to minimize the shading of the cell), and bus lines are introduced where copper tabs will be soldered to extract the current from the cell. Alloying and screen printing techniques are used [1, 5, 6, 21, 22].

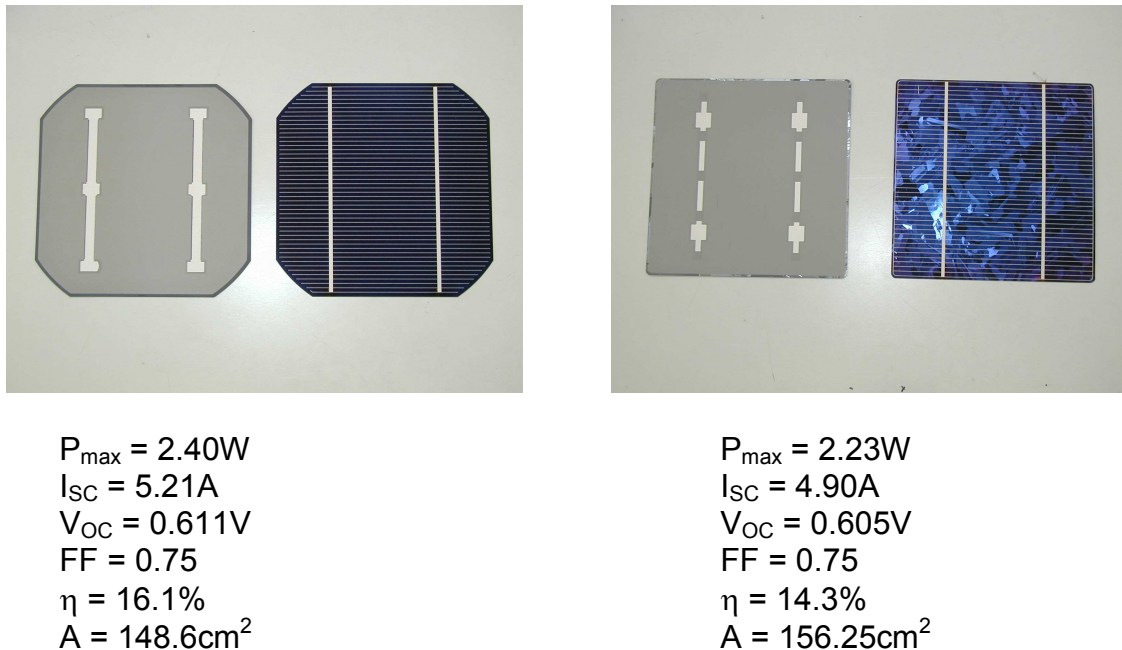


*Figure 2: Monocrystalline and polycrystalline silicon solar cells. Grid lines and bus lines to extract the current from the cell are easily spotted at the front and back of the cells. Specification details are given for the cells (see next subsection for definitions of the parameters).*

Silicon cells are among the most developed cells, with efficiencies of 16% in the case of monocrystalline solar cells and 14% for the polycrystalline cells. Figure 2 presents the back and front faces of monocrystalline and polycrystalline silicon cells (125mm x 125mm), where the horizontal grid lines gathers the current, and the vertical bus lines, where the ribbons or tabs will be solder, are used to extract the current from the cell. The visual effect of the polycrystalline cells is because of the different crystallographic orientation of the polycrystals in the cell. The boundaries of the polycrystals is a source of recombination, although passivated, this reduces the efficiency of the cell in comparison with the monocrystalline ones. Typical data for both kinds of cells are given in Figure 2, as well.

Other cells are made of III-V elements, as Gallium-Arsenide (GaAs), with a gap of 1.43eV, used for concentrator systems due to its direct gap properties, which

ensures a higher efficiency, or Gallium-Antimonide (GaSb) used for Thermo-Photovoltaic (TPV) applications due to its small gap, 0.72eV, suitable for the absorption of IR radiation coming from high-temperature furnaces, etc [22, 21]. Other elements can be alloyed with these semiconductors to improve the characteristics of the solar cells, e.g., customization of the gap, by introducing a fraction of Aluminum,  $\text{Al}_x\text{Ga}_{1-x}\text{As}$ . III—V solar cells are specialized cells, due to its high cost and elaborated production process. They can even be combined in tandem-cells or multijunction cells, which ensure a more efficient absorption of the sun spectrum, reaching a 30% efficiency.

New generation cells, known by the generic name of Thin-Films, are under development and pilot productions are commercialized. These are cells as Cadmium-Telluride (CdTe), Cadmium-Sulfide (CdS), Copper Indium Diselenide (CIS) and others made of II-VI elements. Hope is put on these new materials, with reported efficiencies of 10%, since their production yield may reduce the cost of the modules due to their thinness, 50 $\mu\text{m}$  (compared with 300 $\mu\text{m}$  of Si cells). Another advantage is that they do not require an encapsulant at the front face, increasing the light reaching the active junction and reducing the module production cost [22, 21]. New amorphous silicon cells, passivated with Hydrogen (a-Si:H), are also gaining terrain with wafers of 50 $\mu\text{m}$  and reported efficiencies of 5-6%, near the range of regular thin-film cells [23].

### 3.1.2 Fundamentals of solar cells

As described above the solar cell is in fact a diode working in reverse bias. A diode is an electronic device which allows the conduction of current in forward bias, with an exponential activation as the forward bias is increased, and a constant small current being let through in the reverse direction known as “reverse current” [19, 20]. When one of these devices is illuminated a photo-generated reverse current  $I_L = I_{SC}$  is added to the typical diode current. The behavior of the solar cell is defined by its I-V characteristics, which shows the current generated for a given voltage:

$$I = I_{SC} - I_0(e^{eV/kT} - 1),$$

where  $I_0 \sim e^{-E_g/kT}$  is known as the “reverse current” and has an exponential activation with temperature.

Figure 3 shows a typical I-V characteristics for a typical silicon solar cell, with a short-circuit current  $I_{SC} = 5\text{A}$  (current for  $V = 0\text{V}$ ) and an open-circuit voltage  $V_{OC} = 0.5\text{V}$  (voltage for  $I = 0\text{A}$ ). The power generated at each point by the cell is shown as well in Figure 3. Since the current and voltage vary within ranges 0 and  $I_{SC}$ , and  $V_{OC}$  and 0, respectively, there exists a point in the characteristics which maximizes the power, called “Maximum Power Point (MPP)”, given by  $I_{MPP}$  and  $V_{MPP}$  (the red open circle in Figure 3 on the knee of the characteristics). When the cell is connected to a resistive load ( $V = IR$ , a straight line with a slope  $1/R$ ), the working point of the cell is the intersection of both curves. Ideally the cell should be working at its MPP.

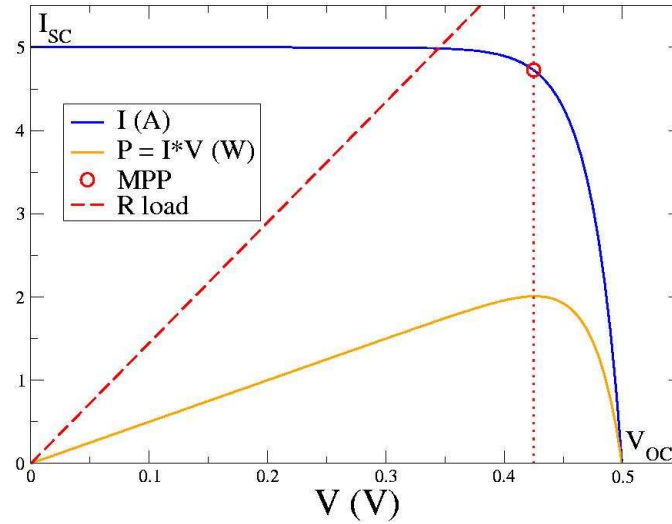


*Figure 3: I-V characteristics for a solar cell. Representation of the current and the produced power in terms of the voltage. The open circle in the I-V characteristics denotes the current-voltage point for which the generated power is maximum, known as Maximum Power Point (MPP). The working point of the cell is given by the intersection of its characteristics and the characteristics of the connected load.*

The cell output is optimized when working at its Maximum Power Point. The MPP has a value of the current and voltage close to those of  $I_{SC}$  and  $V_{OC}$ , and how close they are is determined by the squareness of the characteristics. The Fill Factor (FF) is a measure of the squareness of the characteristics, and it is defined by

$$FF = \frac{I_{MPP} V_{MPP}}{I_{SC} V_{OC}} < 1.$$

The larger the value of FF the better the performance of the cell, with typical values in the range 0.7-0.8. Another parameter defining the performance of the cell is its efficiency,  $\eta$ , given by the ratio of the produced power over the incident power of the light shed on the cell. Typical values vary, and for silicon cells it is about 15%.

The current generated by a solar cell is proportional to the intensity of incident light, and therefore the short-circuit current depends on the available intensity of light (which when mounted in a system depends on shading, cloudiness, angle of incidence of light on the cell, etc.) Figure 4 shows how the I-V characteristics is affected by light intensity: the short-circuit current is reduced with reduced light intensity, reducing, in turn, the generated power. On the contrary the open-circuit voltage is not dramatically affected by light intensity.

The open-circuit voltage is affected, however, by the operation *temperature* of the cell: as temperature increases the exponential thermal activation of the cell reverse current ( $I_0 \sim e^{-E_g/kT}$ ) picks up faster and faster, reducing the value of  $V_{OC}$ , while keeping the value for the short-circuit current virtually unchanged (a slight increment of  $I_{SC}$  is due to the increment of carriers with temperature). This behavior can be observed in Figure 5.

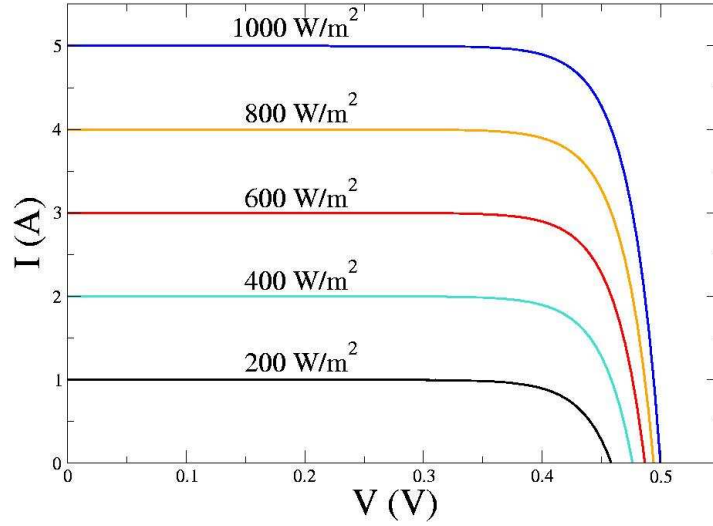


Figure 4: I-V characteristics dependence on light intensity. The proportional dependence of  $I_{SC}$  on light intensity is shown by a reduction of the current as the light intensity is reduced. The open-circuit voltage is slightly reduced even after a large reduction of light.

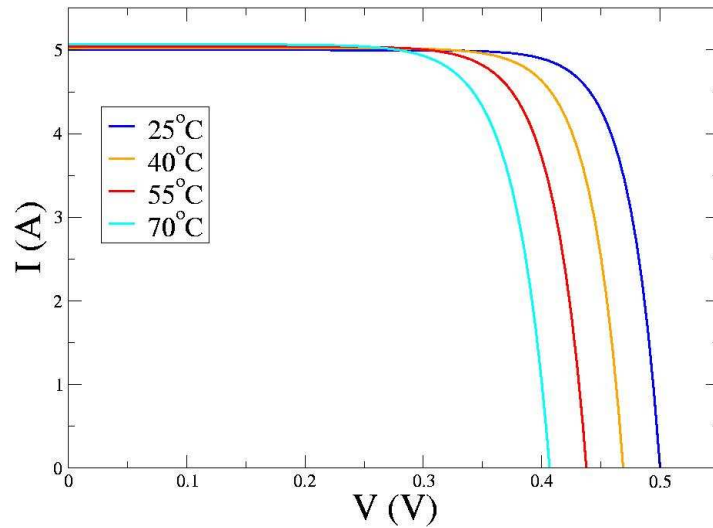


Figure 5: I-V characteristics dependence on temperature. The thermal activation of the reverse current  $I_0$  produces a lower open-circuit voltage, and reduces the power of the cell. The value of the short-circuit current is not affected much by temperature.

The variation with temperature for current, voltage, and power is expressed in terms of the temperature coefficients  $\alpha$ ,  $\beta$ , and  $\gamma$ , respectively, with typical values  $\alpha \sim +0.03\%/^{\circ}\text{C}$ ,  $\beta \sim -200\text{mV}/^{\circ}\text{C}$ , and  $\gamma \sim -0.5\%/^{\circ}\text{C}$ . Since the current, and therefore the power depend on the cell size there coefficients are offered as a relative value, while the voltage depends only on the cell type, and its coefficient is given as an absolute value.

As a consequence of the previous considerations the best performance of the solar cell is obtained with high light intensity and low temperature values. This is difficult to obtain, since a cell exposed to the sun light is absorbing the IR radiation

which excites vibrational modes increasing its temperature. In addition to this there is a thermalization of high energy excitations (much larger than the gap) which increase as well the temperature of the cell. The Standard Test Conditions (STC),  $1000\text{W/m}^2$  and  $25^\circ\text{C}$  of a global AM1.5 spectrum, are a good approach to the maximum performance of the cell, but quite optimistic in order to estimate the output of a solar system in the field.

Another factor affecting the performance of the solar cell is the series resistance (parallel resistance can be considered, but is usually not as important as the series resistance). The existence of a series resistance implies that the voltage drop measured at both sides of the cell does not correspond to the potential drop in the junction. Thus, the external voltage must be corrected such that the cell operation voltage  $V_{op} = V + IR_s$ , where  $V$  is the external applied potential,  $R_s$  is the series resistance, and the positive sign is due to the fact that the generated current  $I$  is, in fact, a reverse current, and negative itself from the usual electrical conventions point of view. Therefore the modified I-V characteristics to take into account the series resistance is given by

$$I = I_{SC} - I_0(e^{e(V+IR_s)/kT} - 1).$$

Figure 6 shows the I-V characteristics for a solar cell with different values of the series resistance. It can be appreciated how the voltage of the MPP reduces as  $R_s$  increases (the MPP corresponds to the open circles on the knee of the curves). The high voltage (around  $V_{OC}$ ) linear behavior is a signature of serial resistance.

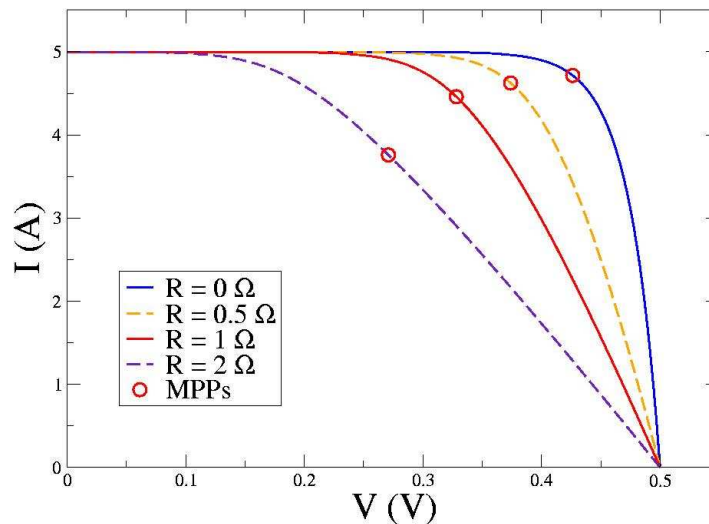


*Figure 6: I-V characteristics dependence on series resistance. The increasing value of the series resistance reduces the power produced by the cell. The open circles represent the MPPs for each characteristics. Linear behavior of the characteristics around  $V_{OC}$  indicates series resistance.*



### 3.2 Solar modules

Solar cells connected together to form modules can be connected in series (configuration known as *string*), which will increase the open-circuit voltage,  $V_{OC}$ , of the module as the number of cells in the string increases (see Figure 7), or in parallel, which will increase the current generated by the system proportionally to the number of cells connected in parallel (see Figure 9).

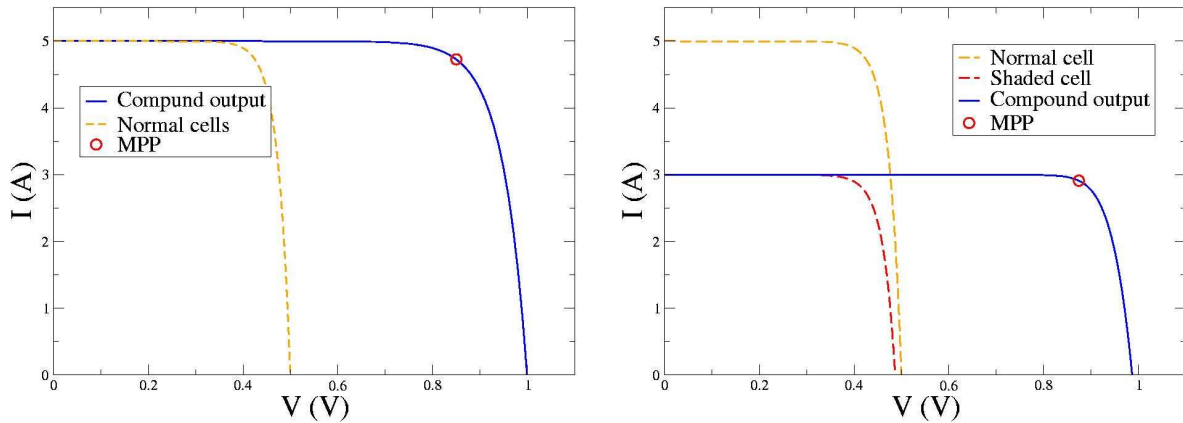


Figure 7: I-V characteristics for a series configuration. The composition of two normal operating cells is shown on the left, giving a larger value for  $V_{OC}$ . On the right a shaded cell hinders the total output of the system.

In the series configuration the operation voltage of two different cells is added up for each value of the current, as it is shown in Figure 7. Therefore by adding an increasing number of cells to the circuit large voltages can be achieved (see Figure 11, for a module characteristics with 126 cells).

One of the major problems which reduce the ideal output of a module is shading. When a cell is partially shaded its characteristics is shifted downwards, producing a smaller current (see Figure 4). When one cell connected in series is shaded, since the rest of the cells are still producing a higher current, and the same current passes through every cell of the string, the shaded cell is forced to work in reverse bias to achieve such current levels. This means that the cell is consuming energy from the system (operating at negative voltage, see Figure 8), lowering the overall output of the system (see Figure 7). In this case it is desirable to by-pass that cell with a diode in parallel, which allows the transport of the required current with minimal losses to the system.

A by-pass diode is connected in parallel with the cell to prevent the reverse bias working point in case of shading. On the I-V characteristics the dashed lines correspond to the normal and shaded cells (the reverse break-down voltage is shown) and the continuous line is the overall output of the string.

Figure 9 shows the output of two solar cells connected in parallel. In this case the current of the cells is added up for every value of the voltage. Again, by connecting several cells in parallel a circuit generating higher currents can be achieved. In general circuits with high currents are not desirable, since the losses

produced by Joule effect go as  $I^2R$ , which means that doubling the value of the current produces four times more losses.

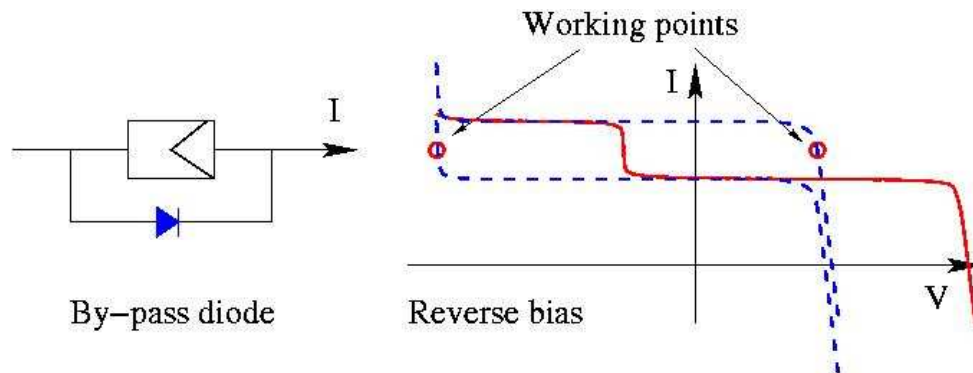


Figure 8: Shaded cell by-pass diode.

As noticed from Figure 9 the effect of shading of a cell in a parallel circuit is not as dramatic as for the series configuration, for the only problem is a reduced contribution of that cell, while not producing losses to the system.

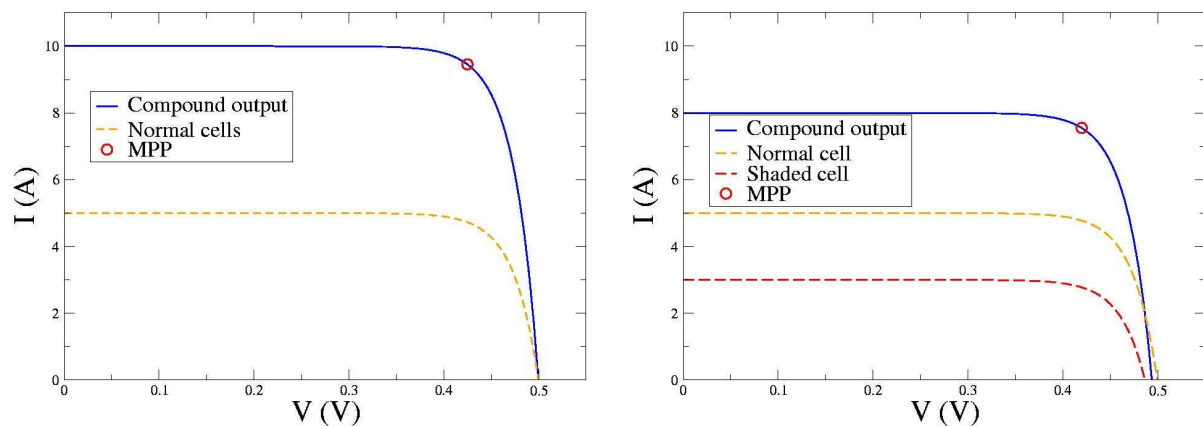


Figure 9: I-V characteristics for parallel configuration. The composition of two normal operating cells is shown on the left, giving a larger value for  $I_{SC}$ . On the right the shaded cell still contributes to the total output of the system despite its smaller output.

### 3.2.1 Glass-glass modules produced by Romag Ltd.

Solar modules are produced by connecting several cells together with one of the configurations above, or even a combination of both. Standard silicon modules are formed by as many as 72 cells connected in series by copper ribbons or tabs (coated with tin/lead), running from the back face of one cell to the front face of the next one in the string (usually for silicon cells the front face has a negative character, while the back face has a positive character, and therefore running the tab from back to front gives the correct direction of the current) laminated with a front glass, EVA (ethylene vinyl acetate) as encapsulant, and a back cover of Tedlar. This

configuration yields a short-circuit current of about  $I_{SC} = 5A$  and an open-circuit voltage of  $V_{OC} = 44V$ , with a maximum power of 150-170W.

Romag Ltd. produces custom-made glass-glass modules for building integration applications, which means that the modules are made of glass at the front and the back, giving a semi-transparent character to the module defined by the cell spacing. The cell spacing determines the “transparency” of the module, given by the rate of the cells covered area to the module surface. Two different constructions for the produced modules are presented in this report: single-glazing and double-glazing constructions.

Figure 10 shows the electric design, with a 9 x 14 array of monocrystalline silicon cells connected in series, with a 3mm cell spacing, of a single glass-glass module of 1.950m x 1.255m of size, with a glass construction of a 4mm thick patterned glass on the front (pyramidal carved for light trapping) and a 6mm blue glass on the back. The transparency of the modules is 23.5%. Thirty of these modules are installed on the façade of the Gateshead International Business Centre in the UK.

By-pass diodes are laminated inside the electric circuit, in parallel with two strings of cells (a whole run of cells going upwards and downwards), as it is illustrated in the close-up detail in Figure 10. Bus bars along the bottom edge of the module gather the current taking it to the junction box through a hole on the back glass, where plug-and-socket connectors are used for easy electrical connections.

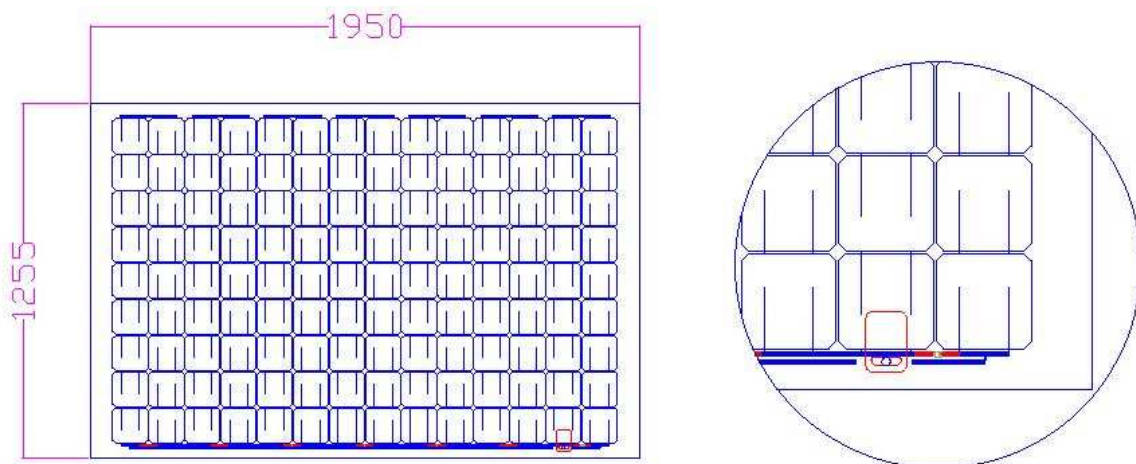


*Figure 10: Single-glazing construction, Gateshead modules. An array of 9 x 14 monocrystalline silicon cells with a 3mm cell spacing and a 23.5% transparency. By-pass diode by-passing every other string in the configuration. A detail of a by-pass diode and the junction box is shown on the right.*

The I-V characteristics of one of these modules is presented in Figure 11, with a MPP power of 294W; very good when compared with the cell performance which would yield 302W without any encapsulation losses (the losses for this module are 2.6%). The  $I_{SC} = 4.80A$ ,  $V_{OC} = 78.03V$ ,  $I_{MPP} = 4.50A$ ,  $V_{MPP} = 65.39V$  and  $FF = 0.79$ . The typical output for these thirty modules is about 265W, with a  $FF = 0.72$ .

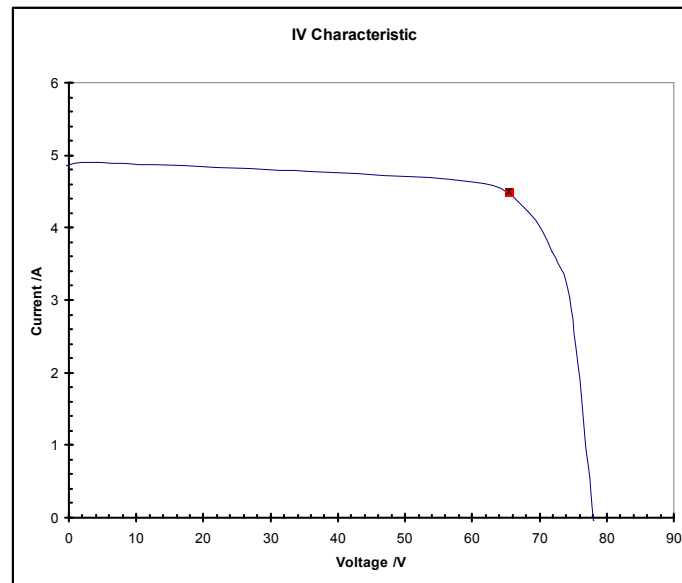


Figure 11: I-V characteristics for Gateshead module.  $I_{SC} = 4.80A$ ,  $V_{OC} = 78.03V$ . The red dot denotes the MPP, with  $P_{MPP} = 294W$ .

Six more modules, doubling the size of the one presented here, will be used as a canopy above the main entrance of the building, with a 12mm glass on the front and a 6mm glass on the back. Not the ideal glass construction, for the thickness of the front glass reduces the intensity of light reaching the cells. Indeed, these modules produce an  $I_{SC} = 3.20A$ , a 33% lower than those with a 4mm patterned glass.

The electric configuration for another order is shown in Figure 12, with 48 polycrystalline cells in series (8 x 6 string configuration), a 10mm cell spacing, and a transparency of 27.5%. This is a double-glazing unit, laminated between two 4mm glasses, installed in the Falstone Tea Rooms in the UK. Other modules with a slight different configuration were produced for the same order.

Once the module is laminated it is taken to be double glazed, where a metallic frame 10mm wide is placed behind the module, and a secondary glass is positioned at the back, leaving an air gap which improves the insulation properties of the module, to be installed in exterior façades. Since the frame is not placed right to the edge of the module it is possible to hide the by-pass diodes, and the external connection leads on the edge of the whole unit (in stead of laminating them in between the glasses as in the previous example), eliminating the need for a junction box and holes on the back glass. Since the edge is filled with silicone all the electric connections are perfectly insulated.

In Figure 12 a diagram of the module, with a front view and the edge view is presented, where the shaded edge of the module marks the thickness of silicone to seal the double-glazed frame from outer weathering. A diagram of the double glazing construction (side view), with the module construction (glass/EVA/cell/EVA/glass), as well as the insulating air gap and back glass is presented on the right hand side of Figure 12. The position of the diodes is shown in the same diagram.

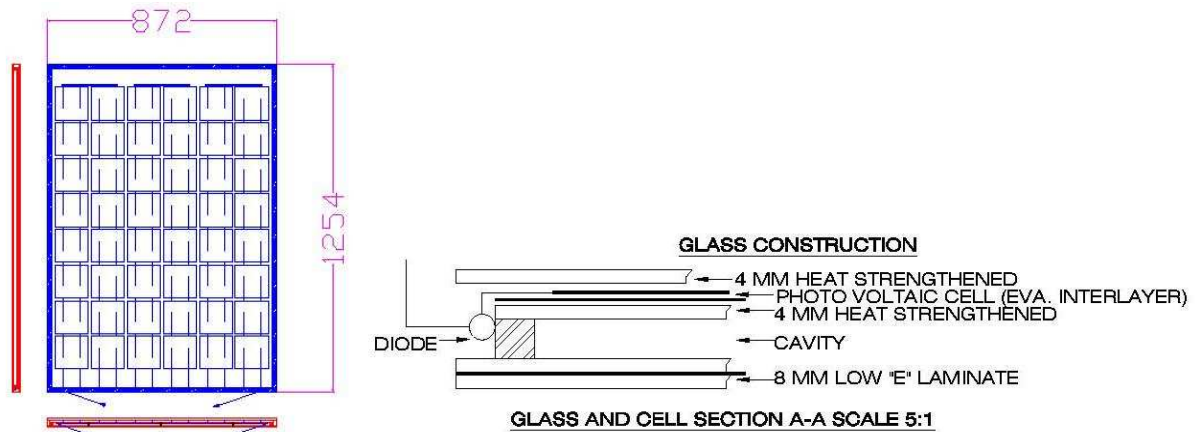


*Figure 12: Double-glazing construction, Falstone modules. A 6 x 8 array of polycrystalline cells, with a 10mm cells spacing and a transparency of 27.5%. Bypass diodes and external leads are hidden on the edge of the double-glazing. A side view of the double-glazing construction is shown on the right.*

The power of these modules is  $P_{MPP} = 106.8W$ , to be compared with the ideal one, 107W, which amounts to a 0.18% of encapsulation losses. Typical values for the performance parameters are  $I_{SC} = 4.70A$ ,  $V_{OC} = 29.72V$ ,  $I_{MPP} = 4.36A$ ,  $V_{MPP} = 24.50V$ , and  $FF = 0.77$ .

### 3.3 Solar systems: Building Integrated Photovoltaic Systems (BIPV)

Once the solar modules are constructed, they are installed in systems by connecting them in a series and/or parallel configuration, known as PV arrays. The current produced by the array is used to power a different range of loads controlled by several devices, known as Balance of Systems (BOS), and they are slightly different depending on the kind of system. PV systems can be classified in two main categories: stand-alone (off-grid) systems and grid-connected systems.

Stand-alone systems consist of the PV array, a bank of batteries, the load to be met by the system and a Power Conditioning (PC) system, which includes a Maximum Power Point tracking system, a Charge Regulator, which controls the charging and discharging of the batteries, and an Inverter to transform the continuous current (DC) produced by the array into alternate current (AC) necessary for some of the loads. A diagram of such a system is presented in Figure 13. The loads usually consist partially of DC loads (illumination systems, and special appliances) and AC loads. It is advisable to use as much of the power in DC, since the inverter has an efficiency of about 90%, losing, this way, 10% of the power in the transformation and reducing the delivered power to the loads. The section and length of the wires must also be carefully chosen in order to minimize the losses.

When the array does not produce enough energy to meet the load a bank of batteries is used by the power conditioning system to deliver the required energy. These batteries have been previously charged from the PV array at moments when the energy demand was below that supplied by the modules. The charge and

discharge process of the batteries implies some losses, as its efficiency is about 90% for each one, leading to an efficiency of the overall process of the 80%. A carefully designed system can work autonomously for long periods of time (until some of the components needs for maintenance or replacement, usually the batteries have the shortest life-cycle).

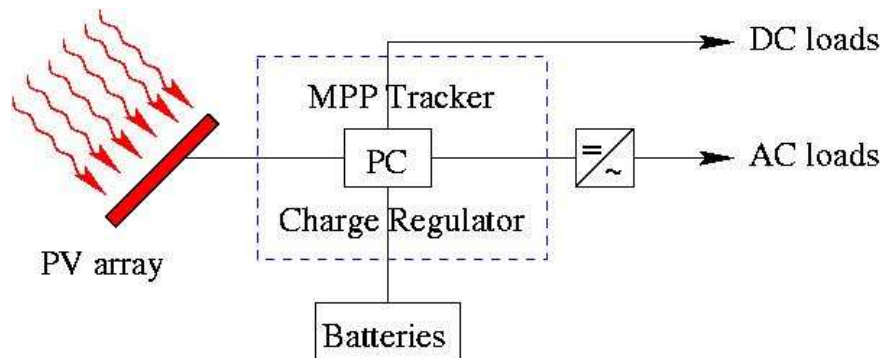


*Figure 13: Stand-alone system diagram. The power generated by the PV array is controlled by the power conditioning (PC) system, which determines if it is delivered to the loads or stored in the batteries.*

Grid-connected systems are installed there where a grid is available, and instead of storing the generated energy in batteries, as in a stand-alone system, this is exported to the grid. Usually they are designed to generate the maximum possible power.

The simplest of all systems generates the power exporting it to the grid through an inverter synchronized with the grid, and the use of a transformer to meet the voltage requirements of the grid (it may be integrated in the inverter). These systems are installed by utilities to meet peak demand and support the grid in remote areas. The installation of this kind of systems is soaring due to the PV promotion schemes, since feed-in tariffs paid for the exported energy are profitable in comparison with the rates paid for the consumed electricity.

Ideally more sophisticated designs use the grid as a storage device, meeting the internal demand of the building or facility where they are installed, in form of DC and AC loads, in the first place, and only exporting the extra energy generated. A system like this is schematically represented in Figure 14.

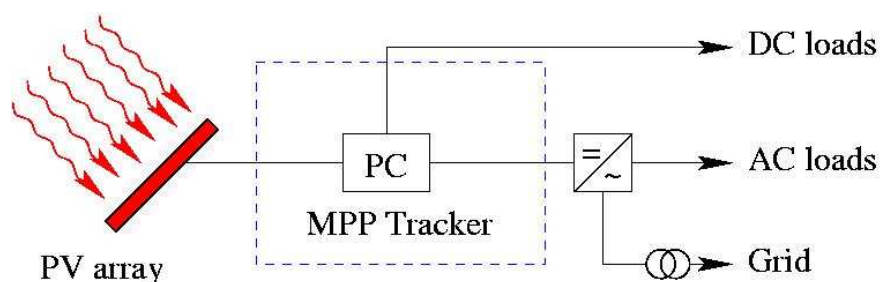


*Figure 14: Grid-connected system diagram. The power generated by the PV array is controlled by the power conditioning (PC) system, which determines if the power is delivered to the loads or exported to the grid. If no internal loads are met all the produced electricity is exported through the inverter to the grid.*



Grid-connected systems are driving the market expansion of PV systems, and more concretely Building Integrated Photovoltaic Systems (BIPV). Modularity of PV systems allows for a step by step installation by replacing old construction materials as the demand grows or systems are more affordable. The fact that this particular kind of application is suitable for installation in the urban environment encourages urban regeneration.

The integration of PV modules and construction materials reduces the price of the system. The cost of a PV system includes cells, circuit design, encapsulating materials (glass, EVA, Tedlar, and frames), and processing of the modules, as well as the BOS and required wiring. In addition to this the installation cost of the system in an existing building or facility must be taken into account. However, laminating a solar cell circuit inside a window the cost of the encapsulating materials is eliminated, since those elements needed to be installed in any case. Moreover, if these windows are installed in the building during the construction stage, the installation cost can be eliminated as well. Yet there is a cost for the BOS, but again its installation is reduced if it is planned and installed during the construction stage.

Examples of building integrated elements are solar tiles for roof mounted systems, cladding elements for the façades, and mainly windows and canopies, which at the same time act as architectural structures playing with the transparency of the modules. Being a glass processing company this is the main production focus of Romag Ltd., and the installation and process definition stages for the glass-glass solar modules in this company is presented in the next sections.

## **4 Production line description**

The production line at Romag Ltd. is partially automated. As explained above, the objective of Romag is to offer custom-made glass-glass modules for building integration. This makes difficult the standardization of the production line, since the number of modules to be produced for each order is limited, and at the same time variable in size and string layout. In order to meet these requirements it is convenient to perform manually some of the assembly tasks, while others can be easily and more conveniently carried out by an automated process [2, 3, 4, 7, 8, 9]. Here a brief overview of the whole process is introduced, which will be described bellow in more detail.

Plots like those shown in Figure 10 and Figure 12 are produced to define the glass size and hole position, if any is required. The position and orientation of the by-pass diodes and the junction box are determined. These drawings allow for an easy operation during the production stage. The glass is ordered according to the specifications given on the drawings and once in the workshop it is washed to ensure all dirt and impurities are eliminated before laying the cell strings.

The production line starts with a cell tester, which checks the output of the cells and their I-V characteristics before stringing them. After that, a complicated and involved piece of equipment, the tabber and stringer, strings the cells, cutting tabs to correct length and soldering the cells together to the desired string length and

cell spacing [7, 8]. Previous to the tabber and stringer there is a fluxing station, which coats the tab with flux, a substance which ensures a correct soldering of the tabs to the front and back surface of the cells.

Once the string is produced a string handler picks the string and places it in position on the glass with a sheet of EVA. This string handler is able to rotate the strings 180° allowing for an alternate layout to produce a continuous series circuit [7, 8]. Due to the non-standardization of the inter-string spaces the bus bars connecting the different strings are manually soldered. At this stage of the process, laminated by-pass diodes are soldered within the circuit (in the case of double-glazed modules by-pass diodes are connected after lamination). The serial number is also placed at this point. The circuit must be inspected for open-circuits, the back sheet of EVA laid and the upper piece of glass is carefully adjusted.

The excess of EVA hanging out of the glass is trimmed before introducing the module in the laminator for the lamination and curing cycles. The lamination cycle melts the EVA, allowing for a perfect adhesion to cells and glass. After the lamination is completed pressure is applied on the laminate and the curing takes place producing cross-linking of the EVA [12]. At the end of this cycle the module is taken out of the laminator and placed under several fans which cool it down.

When the module is cold enough it is taken out of the cooling chamber, the excess of EVA, flowing out of the laminate during the lamination process, is removed, and the junction box, if necessary, installed (for standard modules automated processes have been developed [3, 4]). (Double-glazed modules are taken to the double-glazing unit for the by-pass diodes and external leads to be connected.) The module is placed on a standing support and transported by rollers to the dark testing room, where a flash lamp produces a flash during which a measurement of the I-V characteristics is carried out.

#### **4.1 Cell tester**

This machine tests the electrical output of the individual cells with a high power lamp of Xenon and several filters and pin-holes in a temperature controlled area, in order to simulate as close as possible the Standard Test Conditions: 1000W/m<sup>2</sup> of a global AM1.5 spectrum at 25°C. The lamp is behind a shutter, which is released by the operator to perform the measurement.

In order to obtain accurate measurements a calibrated cell must be used as reference to adjust the power of the lamp. It is convenient to perform this adjustment a couple of times during the day to make sure there are not variations due to daily cycle temperatures. The cell to be calibrated must be exposed to the sun light outdoors to eliminate the initial degradation, after which the cell behaves in a much more stable way. This light induced degradation may amount to a 1-5% of the initial power [24]. In fact, given the fragility of the cell it is advisable to produce a set of secondary calibrated cells to be used regularly as reference during production, and just utilize the primary one seldomly.



The calibration of the lamp is easy, but must be carried out carefully. With a light sensor (a small piece of cell, where tabs have been soldered, will make the function) connected to a multi-meter, a tuning of the uniformity of light is performed. The uniformity is controlled adjusting the X, Y and Z position of the lamp by searching for the maximum current produced by the sensor.

Once the cell tester is calibrated the different packs of cells can be sampled, just to ensure that the data provided by the cell manufacturer is within the specifications. The tester offers several parameters: short-circuit current, open-circuit voltage, and maximum power point current, voltage and power. All these data are shown numerically and in a graph similar to that in Figure 3.

## **4.2 Tabber and stringer**

The stringing of the cells starts with a flux station. This station coats the tabs or ribbons, made of copper coated with tin/lead (60/40), with flux to ensure a good soldering during the stringing process. Up to four reels of tab can be mounted and passed through a tank full of flux, to be rolled at the end in other four reels ready to be mounted in the stringer.

The stringer consists of a conveyor belt cell loader, a sliding linear platen with fingers, a four-axis robot ( $x, y, z, \theta$ ), a tab transfer tool (TTT) and low tab holder (LTH), a cell support and halogen lamps for the soldering (see Figure 15). These subsystems are actuated by independent servos controlled by a main program which synchronizes them to produce the string of cells with the desired cell spacing ready to be laid on the module [7, 8]. The maximum string length is 2 meters, and can contain up to 15 cells.

The tab is dispensed by previously fluxed reels, and cut to a length consistent with the cell size and cell spacing to go from below one of the cells to above the next one in the series. For these to be performed properly when small cells spacing is in use the tab is crimped at half way. Then the TTT picks the tab by means of a suction system and transfers it to the cell support. Once the tab is in place the robot gets one of the cells from the box located on the conveyor belt and lays it sunny-side-down on the cell support. This way the front surface of the cell is in contact with the tab, and the tab transfer tool places a second tab on the back surface of the cell. When the cell and the two pieces of tab are in place the fingers of the platen move forward and hold the tabs in place, moving the block one step forward, such that the robot can place the next cell and a new piece of tab can be laid. This way the string can be completed by repeating these simple steps as many times as cells in the string.

The robot uses a suction system to pick up the cells from stacks of cells in the boxes located on a conveyor belt. This conveyor belt is used, together with the boxes, to provide a continuous supply of cells to the robot, as when one of the boxes is empty, the system automatically removes that one and replaces it by a new one previously loaded by the operator from outside with no interaction with the process at all. In order to make sure that the robot picks one and only one cell the stack of cells is lifted and an air knife is used from the sides to separate possible stuck cells. Once

the robot has picked the cell from the box it presents its sunny-side to a vision camera for visual inspection and determination of the actual position of the cell. The camera sends the information to a computer, which looks for the borders of the cell, and the presence of the bus lines, and in case the cell has a wrong orientation, it is rejected, being sent to a rejection box, and continuing the process with the next cell. In case the cell meets the system quality criteria it is placed on the cell support sunny-side down.

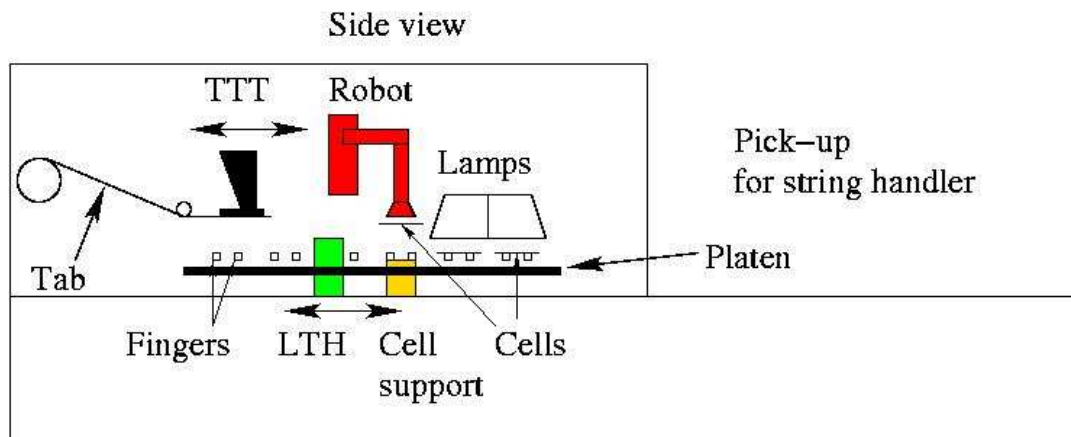


*Figure 15: Tabber and stringer diagram. The different elements, tab transfer tool (TTT), low tab holder (LTH), cell support, robot, and lamps, work synchronized to produce a string of cells.*

As commented above, once the block tab-cell-tab is in place on the cell support the fingers of the platen hold the block and the platen moves forward. The cells come under the halogen lamps, which work in two phases: the preheating phase and the soldering phase. So far all the process has been purely mechanical and not much flexibility of the process is given. However the soldering stage involves physical properties for the different materials and must be carefully controlled. The soldering strength of the tabs must be large enough to hold the tab attached to the cell and transmit the current out of the cell, over long periods of time and environmental conditions. At the same time it must be soft enough to accommodate the different expansion rates of cells, tabs and encapsulant, for them not to break the cells [7, 8, 24].

The preheating and soldering stages are formed by the same set of lamps, whose power during the process, idle power, and heating gain must be adjusted to obtain the appropriate heat profile allowing for the optimum soldering. For example, the preheat stage warms up the cell such that it will not suck heat from the tabs during the soldering stage, leading to an incorrect solder contact. The setting temperatures of the lamps is monitored and controlled by a pyrometer underneath the cell which performs IR readings of the cell temperature close to the tab. When the setting temperature is reached it is maintained by a certain amount of time, controlled by the program, until the soldering is completed.

Cell after cell passes under the soldering lamps until all of them are soldered, and then the platen moves the string away to a position where the string handler will pick it up to lay it on the module.

### 4.3 String handler

The string handler consists of a bar parallel to the platen (and therefore the string) with suction fingers which removes the string from the pick-up position of the platen, shows the front-face of the cells to the operator to check that the tabs are properly soldered and aligned, and, if accepted, places the string on the module (if rejected, the string is placed on a rejection tray, where can be repaired, to be picked up again and placed on the module) [7, 8]. The bar of the string handler can rotate 180° in order to construct a continuous series electrical circuit (Figure 10 and Figure 12) as it is shown in Figure 16.

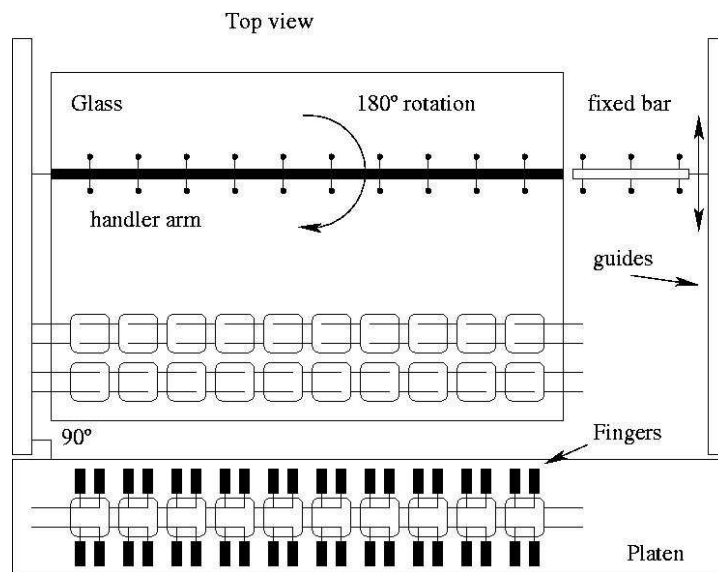


*Figure 16: String handler diagram. The handler bar is parallel to the platen and moves perpendicular to it. The possibility of rotating the string 180° allows for the formation of continuous series circuits.*

The positioning of the string is an accurate process where the handler bar moves perpendicularly off the platen. The guides along which the handler slides away from the platen need to be as close as possible to the 90° with respect to the platen to avoid any offset of the strings as they are laid farther and farther from the platen.

The edge of the glass is detected by a laser beam, and then the string is laid to a given distance defined by the recipe:  $d = (\text{offset from the glass border}) + (\text{cell size} + \text{cell spacing}) \cdot (n-1)$ , where  $n$  is the number of the string being laid.

Ideally the handler would pick up the string symmetrically centered, and then there would not be any difference between the 0° and 180° orientations. However, that is never the case, and the position of the 180° oriented string must be compensated to account for any deviation from a centered handling.

As explained above the maximum string length for the stringer is 15 cells with a minimum cell spacing of 2mm (2 meters long strings). The handler can handle

strings up to 22 cells. The string handler is divided in to sections, one rotational, with the length of the platen (accounting for 15 cells) and one fixed for 7 more cells, amounting to the maximum of 22 cells. If longer than 15 cell strings are needed it is convenient to produce strings half size of the final string length, position them on the rejection tray, hand-solder both halves and take the complete string from there to its position on the module. For this process to be accurate enough the reference position of the string handler bar with respect to the rejection tray needs to be carefully calibrated.

#### **4.4 Bus bars soldering**

Due to the non-standardization of the cell spacing the soldering of the bus bars, connecting electrically the different strings laid on the module, is performed manually (contrary to the standard production [7, 8]). At this stage by-pass diodes are soldered to prevent malfunction of the modules due to shading (see Figure 8).

The by-pass diodes need to be soldered in the correct direction for them to perform their function. If any single cell stops working within a series module it jeopardizes the whole module production. Then, it is desirable to by-pass the cells such that a faulty cell does not hinder the rest of the module. However by-passing every single cell introduces losses in the circuit, and a balance must be reached which accommodates the likelihood of a loss, as well as the ascetics of the module, since many by-pass diodes imply many bus bars with the corresponding increase in labor as well.

The circuit is tested for open circuit, and proper behavior of the individual strings, with a multi-meter, checking the proportional increment of voltage with the number of strings spanned by the measurement. The serial number is also placed at this stage and laminated within the module. This allows for an individual control of the production process and the record of any incidence under such number.

The back layer of EVA and the back glass are placed to finish assembling the module, taking care that the external leads are not bent, or short-circuiting, at the point where they will be connected to the junction box. In the case of a double-glazed module, all the external leads and diodes are soldered later in the step of the glass, and so all the leads come out of one edge of the module before lamination (see double-glazing construction in Figure 12). The excess of EVA hanging out of the module is trimmed to the edge of the glass and the module is transported to the load bed of the laminator ready for lamination.

#### **4.5 Laminator**

The lamination of solar modules is carried out in a laminator with the structure shown in Figure 17. This is one of the largest laminators installed in the world, and it is capable of laminating modules up to 2.2m x 3.5m, or several modules at once as long as they fit inside the lamination chamber.

The laminator is formed by a loading conveyor belt, the lamination chamber and the cooling chamber [9]. Once the module is inside the lamination chamber the top cover comes down, evacuating the air to approximately 5mbars of pressure. This top cover has a diaphragm with an air bag which can be filled to apply pressure on the module. The bottom plate of the laminator contains the heating elements covered by the Teflon belt. Thermocouples are attached to the center and extremes of the different heating elements to monitor and control their temperature. The temperature control is performed by the thermocouples located in the central position of the heaters. A set of pins lifts the module from the hot plate to prevent the bending of the glass caused by a fast heating, due to the difference in temperature between the bottom and top glass which produces stress in the laminate leading to cell fractures. The thermal mass of the glass loaded produces a lagging in the temperature of the EVA [11]. This implies an indetermination which complicates the lamination cycle.

The lamination and cooling chambers are connected by a single and continuous Teflon belt which carries the module [9]. Once the module has undergone a complete cycle of lamination and curing the top cover lifts and the belt moves the module forward to the cooling chamber, where several fans produce an air flow on the module cooling it down. The loading system allows for the loading of a second module in the lamination chamber while the first one is transferred to the cooling chamber, providing a continuous operation of the laminator. This is very important since the laminator acts as a bottle neck in the production process, with lamination times between 30 and 90 minutes depending on the thickness of the glass being laminated. A detailed explanation of the lamination and curing processes is presented in Section 5.

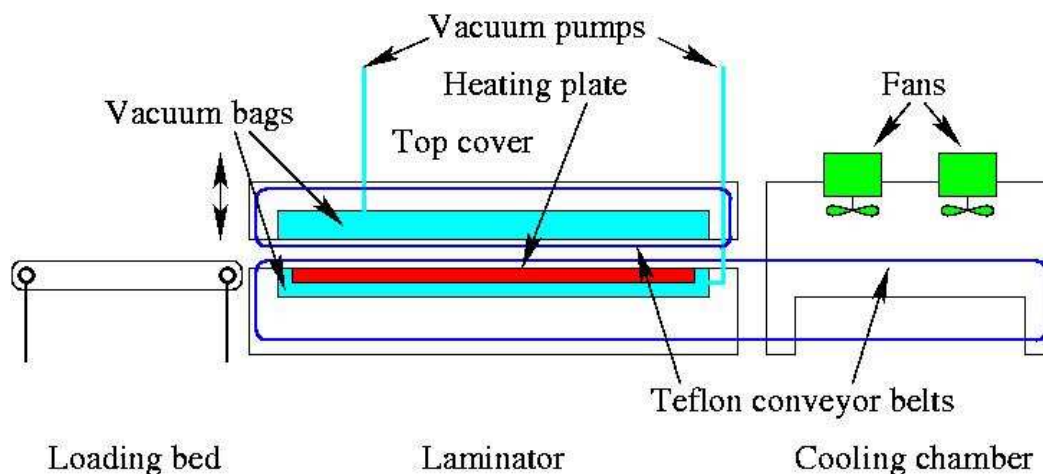


*Figure 17: Laminator diagram. The loading bed loads a module in the lamination chamber, which is connected by a continuous Teflon belt to the cooling chamber. The laminator has a top cover with a diaphragm which applies pressure on the module during lamination.*

#### 4.6 Flash-tester

As explained at the beginning of this section, after lamination the module is cooled down and any overflowing EVA trimmed and cleaned, and connection boxes

are installed at this point (automated processes have been developed for standard module production [2, 3, 4]). Then, the module is left on the rolled bed for it to reach room temperature. It must be taken into account that the inside of the module (where the cells are) takes longer to cool down than the external glass, and it is important that the cells are at room temperature in order to perform an accurate measurement of the module output.

The module is lifted to a standing position resting against a support frame with a slight angle with the vertical. Rollers along the lower part of the support are used to take the module into the tester room. This is a dark room, 13m x 5.3m, with the walls, floor and ceiling painted in black with a special antireflective paint in the IR.

The flash-tester consists of two flash lamps which produce a light intensity above  $1000\text{W/m}^2$  at a distance of 9.6m with a AM1.5 global spectrum [10]. The lamps are positioned pointing perpendicularly to the center of the support frame. This distance guarantees a light uniformity for a reliable measurement of the I-V characteristics for the largest modules laminated, namely, 2.2m x 3.3m.

Electronic sophisticated equipment controls the measurement. When the flash is fired a light sensor detects it and triggers an analog to digital converter to perform measurements of the light intensity, current and voltage of the module.  $I_{sc}$ , and  $V_{oc}$  are registered by a first flash, and the I-V characteristics is scanned by a second flash from  $V_{oc}$  to  $I_{sc}$  with 200 sampling points.

A reference module provides a measurement of the light intensity. The profile of the flash is not uniform during the flash duration, it starts at zero, rapidly increasing to the maximum value, staying stable (plateau) for a period of time and slowly decaying afterwards. The measurements are performed during the flash plateau, where all the intensity points are within the 10% of the maximum. The system optimizes the measurement procedure by making sure that the data is best distributed over the flash plateau.

The output data is corrected to  $1000\text{ W/m}^2$  and  $25^\circ\text{C}$  to meet the STC (Standard Test Conditions). Raw data is transformed, first, to the average intensity of the flash plateau by standard algorithms. Corrections of series resistance are introduced when necessary. If the module temperature is different from  $25^\circ\text{C}$  a temperature correction is performed as a second step. And finally the I-V characteristics is transformed to an intensity of  $1000\text{W/m}^2$ . The data is printed to a graph like that in Figure 11.

## 5 Lamination process

The lamination of the module is the most delicate of all the processes involved in the solar module fabrication. The module construction is shown in Figure 12; the cells and interconnecting ribbons are covered by a layer of the encapsulant material ethylene vinyl acetate (EVA) on the front and the back, and this is covered with two pieces of glass (standard modules are covered by a piece of glass on the front and Tedlar on the back).

The module constructed this way enters the laminator to undergo a cycle of time-temperature-pressure which produces the lamination and cross-linking of the encapsulant. During lamination time there is no control of what is happening with the assembled module, and thus it is necessary to understand the physical and chemical properties of the encapsulant (EVA), and the possible influences of silicon solar cells, metallic interconnections and glass on it [11, 12]. The fact that the laminate has two glasses is relevant, as the thermal inertia of a large volume of glass requires long lamination periods of time for the EVA to reach the required temperatures.

## **5.1 Physical and chemical properties of EVA**

The purpose of encapsulation, as explained by Czanderna and Pern in Ref. 12, is to provide structural support and positioning for the solar cell circuit assembly, to achieve and maintain maximum optical coupling between the solar cell and the incident solar irradiation in the prescribe spectral region with an initial transmission of at least 90%, to provide and maintain physical isolation of the solar cells and circuit components from exposure to hazardous or degrading environmental factors, to achieve and maintain reliable electrical isolation of the solar cell circuit elements from both the operational and safety viewpoints, and to provide electrical interconnections for the cells within a module. Thus, encapsulation provides all necessary functions except for the cell materials and the BOS for conducting the generated electricity from the module outlet terminals. All this requirements must be met for the whole operating period, estimated in 20-30 years.

In order to serve these purposes the encapsulant must be a low cost material, and have good processability, high optical transmission, high dielectric constant, low water absorptivity and permeability, high resistance to UV degradation and thermal oxidation, good adhesion, mechanical strength, and chemical inertness.

EVA (ethylene vinyl acetate) meets the physical, chemical and low cost requirements, and it is the most extensively used encapsulant [11, 25, 26]. EVA is a random copolymer of ethylene and vinyl acetate. For PV applications, the copolymer is 33% in weight of vinyl acetate. A major source of unstabilized EVA copolymer is Elvax 150, manufactured by DuPont, which is susceptible of undergoing photothermal degradation, leading to chain scission and crosslinking reactions. To inhibit these degradative reactions other additives are mixed with the polymer such that when their concentrations are properly balanced, stable EVA formulations are achieved.

The main degradation mechanisms of unstabilized EVA come from chain scission and crosslinking reactions and the function of the additives mentioned above is to reduce this degradation. Cyabsorb UV 531 absorbs UV radiation and quenches excited states (formation of polyenes –unsaturated carbon bonds– and chromophores [27, 28, 29]). Tinuvin 770 scavenges free radicals, and Naugard P is a hydroperoxide decomposer. The stabilized EVA has the following composition [12]:

Elvax 150 <sup>TM</sup>	97.943%	EVA copolymer
Cyabsorb UV 531 <sup>TM</sup>	0.294%	UV absorber
Tinuvin 770 <sup>TM</sup>	0.098%	UV stabilizer
Naugard P <sup>TM</sup>	0.196%	Anti-oxidant
Lupersol 101 <sup>TM</sup>	1.469%	Curing agent (standard curing, A9918)
Lupersol TBEC <sup>TM</sup>	1.469%	Curing agent (fast curing, 15295)

To obtain uncured EVA films suitable for handling but prior to laminating and curing, Elvax 150 pellets, the stabilization additives, and Lupersol curing agent are compounded into a uniform mixture and extruded into films at about 90°C. The resultant films are typically 0.46mm thick packaged into rolls 700-1600mm wide and 100m long.

There are two widely used EVA films, designated by Springborn Laboratories as A9918, formulated with the standard curing agent Lupersol 101, and 15295, formulated with the fast curing agent Lupersol TBEC. If a primer is added to the composition these are named A9918P and 15295P respectively. The initiation activation energy for a given reaction is usually higher than the propagation one, and then a primer reduces the former one speeding the curing process of the EVA. Other advanced formulations have been developed in order to obtain faster curing, with better thermal processing, or to encapsulate other kind of cells [6, 11, 26].

The curing agents, Lupersol 101 or Lupersol TBEC, in the stable EVA formulations are required because Elvax 150 softens to a viscous melt above 70°C, and therefore must be cross-linked for service temperatures greater than 70°C. The degree of cross-linking is expressed as gel content in which the % gel content is an indication of the fraction of the polymer that is not extractable (e.g., with toluene or tetrahydrofuran) and thus is the fraction that is cross-linked. The expected gel content in EVA for different times and temperatures is tabulated [30]. Springborn Laboratories recommend a minimum gel content of 60%, but 80% or above is preferable. Even 100% of gel content does not hinder module performance as long as the encapsulant remains soft and retains reasonable elasticity. The gel content is influenced significantly by the lamination and curing cycle used during module manufacture.

Even stabilized and cured EVA suffers degradation induced by photo, thermal, photo-thermal, acetic acid-catalyzed, and metal and metal-ion catalyzed effects [12, 31, 32]. However, the absolute stability of the encapsulant is not a requirement, as long as the rate of degradation is slow enough not to reduce the expected lifetime of the module. Thermal and photo-thermal degradation mechanisms are the most important ones, as the modules are in the sun receiving heat and UV radiation. Metal catalyzed effects are very important in the laminate, since the EVA and the copper ribbons and cell grid lines are in direct interaction. The effect of copper in catalyzed degradative reactions of EVA have been studied by Willis [33] finding a severe oxidation of the EVA at high temperatures initiated at the metal-EVA interface and propagating through the polymer as a reaction front.



## 5.2 Lamination cycle definition

The lamination process was outlined in subsection 4.5. The module is loaded into the laminator (see Figure 17), the air is evacuated, and the module undergoes a time-temperature-pressure cycle [12]. The temperature is increased from room temperature until it reaches 110-120°C (recall that EVA melts at temperatures of about 70°C), during which the EVA melts and the assembled module is laminated. Given that the laminator has a set of pins which, when lifted, prevent the module from laying directly on the hot plate, the time-temperature ramp can be started at a high temperature of the heating elements, and the module is radiatively heated by the hot plate. Otherwise the bottom glass would heat up too fast as compared to the top glass, producing stresses within the laminate and leading to cell fractures. When the module is hot enough the pins are lowered and temperature continues increasing at a much faster rate, melting the EVA, up to 110-120°C. Then pressure is applied from the top cover diaphragm sticking the module together, as temperature is increased up to 140-150°C to undergo cross-linking during the curing process of the Lupersol agents, 60 minutes for standard-curing Lupersol 101, and about 7 minutes for fast-curing Lupersol TBEC (typical data for standard modules). After that the pressure on the module and the vacuum are released, the chamber is opened and the module is taken out to the cooling chamber, where fans cool it down to room temperature.

The lamination/curing process is quite well established for the lamination of standard modules, and EVA manufactures, as well as laminator manufactures, have recommended values for the time-temperature-pressure setting in this case. However, when the laminate is a glass-glass module (glass/EVA/cell/EVA/glass) the thermal mass loaded in the laminator has a large influence in the heating rate of the EVA, and longer remaining times within the laminator are needed [11]. In Figure 18 a typical profile for temperature and time is presented for the heating elements, the glass (since the heat is received from bellow top and bottom glasses will heat up at a different rate) and the EVA. There is an uncertainty in the temperature of the EVA, which may not even reach the curing set temperature of 140-150°C if the process is no carefully controlled, not obtaining the precise gel content. In addition to this fast cure EVA (15295P) has a tendency to generate bubbles during the lamination because of thermal decomposition of the curing agent Lupersol TBEC to produce CO<sub>2</sub> and other gaseous organics at the curing temperatures [11].

Taking into account that the time for the set temperatures to be reached by the EVA is not well controlled, strongly depending on the thickness of the glass that the module contains, and the possible bubbling problems with the curing agent of the fast-cure EVA, a systematic method must be set to determine the lamination recipes.

The first step is to determine a recipe for a given glass thickness (4mm), to move afterwards to different glass thickness. Secondly, EVA is laminated between two sample glasses 500mm x 500mm (empty module), to determine the lamination and curing time-temperature settings.

Sometimes the module contain bubbles, and in order the determine if these bubbles are produced at the lamination stage or the curing stage, the module can be ejected from the laminator after the lamination cycle (before taking the temperature

to 140-150°C), to inspect the module. Once it is checked that the lamination cycle does not produce bubbles the module is loaded back for the curing cycle.

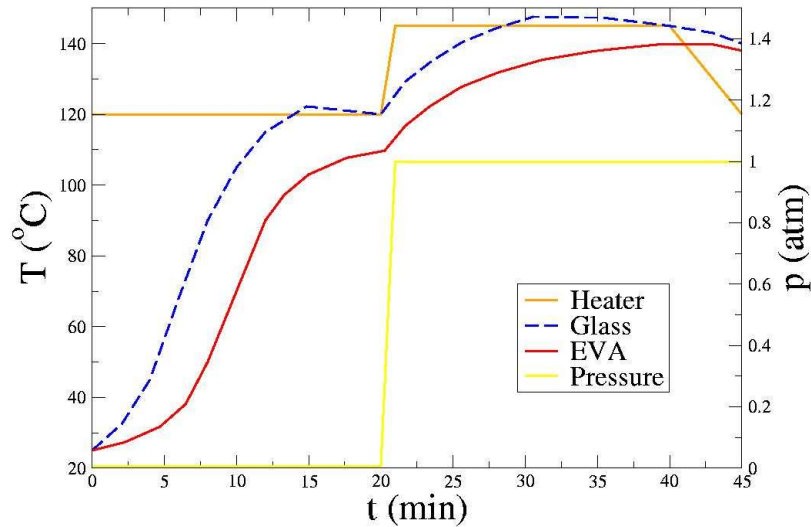


*Figure 18: Lamination process cycle parameters. Temperatures for the heaters, the glass and the EVA are shown. A lagging in the EVA temperature produces an uncertainty in the gel content production. Pressure of the top diaphragm is applied to laminate the assembled module together. Adapted from Ref. 11.*

If not cured enough, independently of the fact that the desired gel content is reached or not, the EVA presents a milky aspect. This problem is overcome by increasing the curing time (or curing temperature). The presence of bubbles at the end of the curing cycle seems to be linked with an over-cooking of the EVA (thermal decomposition of the fast-curing agent Lupersol TBEC), which is mainly due to an excessive temperature. Reducing the curing temperature and increasing the cycle time seems to give better results.

When a reasonable aspect of the empty module (glass/EVA/glass) is obtained, a complete module, with cells and interconnecting ribbons, is loaded into the laminator to fine-tune the recipe. (As for many other physical and chemical reactions the behavior of the materials involved in the processes is modified when by the presence of the other materials.) Most of the times it is necessary to increase the curing time for the complete module, what increases the likelihood of bubble generation. Even when the production of the first modules with a given construction starts, further tuning of the lamination/curing cycle is required. This is due to the fact that while the sample modules are laminated in the center of the laminator, ideally, the laminator is filled at full capacity, and the temperature distribution inside is not perfectly uniform (the edges and corners of the laminator present a lower temperature than that in the center, according to specifications  $\pm 3\%$ ).

As commented above the lamination/curing cycle depends on the thermal mass, i.e., the thickness of the glass, loaded into the laminator. Since the heating elements have to heat the whole assembly up to lamination and curing temperatures, it is reasonable to assume a proportionality rule: a double mass of glass will need twice as much time to reach the required temperatures. This is the first trial in the systematic process defined above when a recipe for new module

constructions has to be defined. If the difference in construction is not very large, the new recipe can be set with two or three lamination trials.

## **6 Conclusions and prospects**

The current international policy environment, after the signing of the Kyoto Protocol, and the subsequent policies passed by the EU and member states supporting the Renewable Energy Sources, is favorable for the expansion of the RES market, in general, and the PV market in particular. The expansion of the PV market, growing at rates higher than 30% per year, is driven by these policies, but also by the fact that PV systems can be integrated in the urban environment and connected directly to the grid. Building integration of PV elements is on the rise because offsets the cost of encapsulation and installation, which accounts for a large amount of the final price of PV systems. With these considerations, it seems natural for an architectural glass processor company to expand their business to cover the production of PV architectural modules.

This report has presented the setting up of one of the newest production lines for custom-made glass-glass PV modules. The commissioning and testing stages of the equipment, as well as the definition of the production process, in which the candidate has had a relevant contribution, were reviewed. The different levels in which man-made solar energy conversion systems are divided, namely, solar cells (mono- and poly-crystalline silicon), solar modules, and solar systems, were thoroughly introduced, paying attention to some problems which may rise due to shading and how to minimize them by the introduction of by-pass diodes. In the module level details were given of the design for two different module constructions, single-glazing and double-glazing. Such that once the design of the module is produced its production can start in the production line.

The production line is partially automated, which allows for an efficient assembly of some of the steps, as the stringing of cells interconnecting them electrically. Due to the custom-made nature of the architectural market (module size, cell spacing) standardization of the production is not completely possible, and some of the stages are more efficiently performed manually.

The process starts with the stringing of the cells to the required length of the string and cell spacing, where a sophisticated piece of equipment connects electrically the cells. Once the string is ready, another machine, the string handler, places the strings in the correct position on the module (glass/EVA). All these strings are interconnected to form a continuous series circuit. By-pass diodes are added to the circuit, if necessary, at this stage. A second layer of EVA and the back glass are placed, and the module is introduced into the laminator to undergo a lamination/curing cycle, which finishes the encapsulation process. When the module is taken out of the laminator and at room temperature it is passed to a dark room where a flash test is performed to obtain its performance output.

During the lamination/curing cycle the module undergoes a very delicate process of time-temperature-pressure, which depends on the properties of the encapsulant material. Care must be taken of this process for the encapsulant (EVA)

not to produce bubbles, while still performing the required functions properly. The encapsulant must provide structural support, optical coupling, electrical isolation, physical isolation/protection, and thermal conduction for the solar cell assembly. EVA, which contains a series of stabilizers, is adequate for these functions since it has a good processability, high optical transmission, high dielectric constant, low water absorptivity and permeability, high resistance to UV degradation and thermal oxidation, good adhesion, mechanical strength, and chemical inertness [25].

Due to the on-going commissioning and setting up of the equipment the production process is not running smoothly enough. In order to improve the process, as well as the quality of the produced modules, an incident record system must be set to obtain any relevant data corresponding to each module. At the end of the process all these data can be gathered together with the performance parameters and the I-V characteristics. The performance losses can, then, be tracked down along the process to determine their origin, modifying whatever procedure is necessary until the best quality is achieved for the product. In this respect the modules must be produced to meet the performance standards IEC-61215 (not all of the standards can be met, e.g., there is no frames for these modules), at the same time that comply with the construction standards of structural support, heat and noise transmittance, etc.

Another line of optimization would be to work in connection with the system designers. That way at the design stage of the modules the strings can be aligned in the electrical circuit in the horizontal or vertical direction, depending on the way shadows cast on the building, in order to minimize the losses. Also the position of the external leads may be defined considering the module arrangement in the PV array, minimizing the wiring length, and reducing, therefore, the losses by Joule effect.

## References

- [1] J. H. Wolgemuth et al., Progress in Solarex crystalline silicon PVMaT program, Proceedings of the 24<sup>th</sup> IEEE Photovoltaic Specialists Conference (1994) 1181.
- [2] M. J. Nowlan et al., Process automation for Photovoltaic module assembly and testing, Proceedings of the 28<sup>th</sup> IEEE Photovoltaic Specialists Conference (2000) 1424.
- [3] M. J. Nowlan et al., Development of photovoltaic module process automation, Proceedings of the 17<sup>th</sup> Photovoltaic European Conference (WIP-Munich and ETZ-Florence) (2001) 743.
- [4] M. J. Nowlan et al., Development of automated Photovoltaic module manufacturing processes, Proceedings of the 29<sup>th</sup> IEEE Photovoltaic Specialists Conference (2002) 414.
- [5] M. D. Rosenblum et al., PVMaT technology improvements in the EFG high volume PV manufacturing line, Proceedings of the 29<sup>th</sup> IEEE Photovoltaic Specialists Conference (2002) 58.

- [6] S. P. Shea and J. H. Wohlgemuth, Improvements to polycrystalline silicon PV module manufacturing technology, Proceedings of the 29<sup>th</sup> IEEE Photovoltaic Specialists Conference (2002) 227.
- [7] M. J. Nowlan et al., Advanced automation techniques for interconnecting thin silicon solar cells, Proceedings of the 24<sup>th</sup> IEEE Photovoltaic Specialists Conference (1994) 828.
- [8] M. J. Nowlan et al., Processing evaluation of an automated high-throughput system for interconnecting crystalline silicon solar cells, Proceedings of the 25<sup>th</sup> IEEE Photovoltaic Specialists Conference (1996) 1331.
- [9] S. J. Hogan et al., Automated lamination for Photovoltaic module encapsulation, Proceedings of the 23<sup>rd</sup> IEEE Photovoltaic Specialists Conference (1993) 1232.
- [10] K. Bücher, Accurate production line testing of high capacity modules, high efficiency modules, and very large area building integrated PV modules, Proceedings of the 17<sup>th</sup> Photovoltaic European Conference (WIP-Munich and ETZ-Florence) (2001) 698.
- [11] F. J. Pern and S. H. Glick, Thermal processing of EVA encapsulants and effects of formulation additives, Proceedings of the 25<sup>th</sup> IEEE Photovoltaic Specialists Conference (1996) 1251.
- [12] A. W. Czanderna and F. J. Pern, Encapsulation of PV modules using ethylene vinyl acetate copolymer as a pottant: A critical review, Solar Energy Materials and Solar cells **43** (1996) 101-181.
- [13] G. Boyle, Renewable Energy: Power for a Sustainable Future, Oxford University Press, Oxford, 1996.
- [14] M. Bess, Market liberalization: Opportunity or threat for renewable energy?, Renewable Energy World (James & James Ltd.), Vol. 2, No. 4 (July 1999) 28.
- [15] D. A. Horazak and J. S. Brushwood, Renewables prospects in today's conventional power generation market, Renewable Energy World (James & James Ltd.), Vol. 2, No. 4 (July 1999) 34.
- [16] P. Appleby, Renewables in the future energy supply, Renewable Energy World (James & James Ltd.), Vol. 2, No. 4 (July 1999) 50.
- [17] P. Huesser et al., Added Value of Photovoltaic Power Systems, Proceedings of the 17<sup>th</sup> Photovoltaic European Conference (WIP-Munich and ETZ-Florence) (2001) 873.
- [18] R. Haas, Building PV Markets: Customers and Prices, Renewable Energy World (James & James Ltd.), Vol. 5, No. 3 (May-June 2002) 98.
- [19] S. M. Sze, Semiconductor Devices, Physics and Technology, (John Wiley & Sons, 1985).

- [20] B. G. Streetman and S. Banerjee, Solid State Electronic Devices, (Prentice Hall, fifth edition, 2000).
- [21] L. D. Partain, Solar Cells and their Applications, (John Wiley & Sons, 1995).
- [22] R. H. Bube, Photovoltaic Materials, (Imperial College Press, 1998).
- [23] P. A. Basore, Pilot production of thin-film crystalline silicon on glass modules, Proceedings of the 29<sup>th</sup> IEEE Photovoltaic Specialists Conference (2002) 49.
- [24] M. A. Quintana et al., Commonly observed degradation in field-aged Photovoltaic modules, Proceedings of the 29<sup>th</sup> IEEE Photovoltaic Specialists Conference (2002) 1436.
- [25] A. W. Czanderna and F. J. Pern, Estimating service lifetimes of a polymer encapsulant for Photovoltaic modules from accelerated testing, Proceedings of the 25<sup>th</sup> IEEE Photovoltaic Specialists Conference (1996) 1219.
- [26] F. J. Pern and S. H. Glick, Improved photostability of NREL-developed EVA pottant formulations for PV module encapsulation, Proceedings of the 26<sup>th</sup> IEEE Photovoltaic Specialists Conference (1997) 1089.
- [27] F. J. Pern, Polymer encapsulants characterized by fluorescence analysis before and after degradation, Proceedings of the 23<sup>rd</sup> IEEE Photovoltaic Specialists Conference (1993) 1113.
- [28] F. J. Pern, Factors that affect the EVA encapsulant discoloration rate upon accelerated exposure, Solar Energy Materials and Solar Cells **41/42** (1996) 587-615.
- [29] F. J. Pern, Factors that affect the EVA encapsulant discoloration rate upon accelerated exposure, Proceedings of the 24<sup>th</sup> IEEE Photovoltaic Specialists Conference (1994) 897.
- [30] E Cuddihy, C. Coulbert, A. Gupta and R. Liang, Electricity from photovoltaic solar cells, Flat-Plate Solar Array Project, Final Report, Volume VII: Module Encapsulation, JPL Publication 86-31 (Jet Propulsion Laboratory, Pasadena, CA, 1986).
- [31] F. J. Pern and S. H. Glick, Photothermal stability of encapsulated silicon solar cells and encapsulation materials upon accelerated exposures, Solar Energy Materials and Solar Cells **61** (2000) 153-188.
- [32] F. J. Pern and S. H. Glick, Photothermal stability of encapsulated silicon solar cells and encapsulation materials upon accelerated exposures – II, Proceedings of the 28<sup>th</sup> IEEE Photovoltaic Specialists Conference (2000) 1491.
- [33] P. B. Willis, Investigation of materials and processes for solar cell encapsulation, Final Report for JPL, DOE/JPL-954527-86/29, August, 1996.